

CERN-PH-EP-2018-D1.0  
April 18, 2018 2018

# $\Sigma^0$ and $\bar{\Sigma}^0$ Production in pp Collisions at $\sqrt{s} = 7$ TeV

PC: A. Borissov, A. Badala, [J. Song](#), I.-K. Yoo  
IRC:

ALICE Collaboration\*

## Abstract

The first measurements of  $\Sigma^0$  and  $\bar{\Sigma}^0$  baryons' transverse momentum ( $p_T$ ) spectra, integrated yields and mean  $p_T$  in ~~pp~~-proton-proton (pp) collisions at the LHC are reported. The  $\Sigma^0$  ( $\bar{\Sigma}^0$ ) signal is reconstructed via the  $\Lambda$  ( $\bar{\Lambda}$ ) +  $\gamma$  decay channel by invariant mass analysis. The  $\Lambda$  ( $\bar{\Lambda}$ ) baryon is reconstructed by its decay into  $p + \pi^-$  ( $\bar{p} + \pi^+$ ), while the photon is detected exploiting the unique capability of the ALICE detector to measure low energy photons via conversion into  $e^+e^-$  pairs. The yield of  $\Sigma^0$  ( $\bar{\Sigma}^0$ ) is compared to that of the  $\Lambda$  baryon, which has the same quark content but different isospin. These data contribute to the understanding of hadron production mechanisms and provide a reference for constraining QCD-inspired models and tuning Monte Carlo event generators such as PYTHIA.

17	<b>Contents</b>	
18	<b>1 Introduction</b>	<b>3</b>
19	<b>2 Experimental setup and event selection</b>	<b>3</b>
20	<b>3 Data analysis</b>	<b>4</b>
21	3.1 Signal extraction . . . . .	6
22	3.2 Corrections and normalization . . . . .	6
23	3.3 Systematic uncertainties . . . . .	7
24	<b>4 Results and discussion</b>	<b>9</b>
25	4.1 Transverse momentum spectrum . . . . .	9
26	4.2 $\frac{\Sigma^0}{\Lambda}$ ratio . . . . .	10
27	<b>5 Conclusions</b>	<b>12</b>
28	<b>A The ALICE Collaboration</b>	<b>16</b>

## 1 Introduction

The study of strange baryons and their resonances in ~~proton-proton~~ ~~pp~~ collisions provides a reference for tuning QCD inspired event generators and contributes to the understanding of strangeness production mechanisms. Colliding projectiles initially contain no strange valence quarks indeed and therefore all strange particles are created in the collisions. In particular,  $\Sigma$  measurements can help to understand production mechanisms of baryons with non-zero isospin. These are an important complement of the ~~Lambda~~  $\Lambda$  data as these particles have similar mass ( $m_\Sigma - m_\Lambda \sim 77$  MeV) and equal quark content (uds), but different isospin value ( $I_\Lambda = 0, I_\Sigma = 1$ ) [1]. Furthermore a yield ratio of  $\Sigma^0$  to  $\Lambda$  can provide a hint to understand a charge and/or isospin independency of the  $\Sigma^\pm$  and  $\Sigma^0$  due to the same  $I(J^P)$ , analogy to the yield ratio of  $\pi^0/\eta$  [2].

All  $\Lambda$  ( $\bar{\Lambda}$ ) measurements include a feed-down from  $\Sigma^0$  ( $\bar{\Sigma}^0$ ). Only the feed-down from weak decays can be corrected for the yield estimation, unless specifically mentioned. In fact, the main decay of the  $\Sigma^0$  ( $\bar{\Sigma}^0$ ) is the electromagnetic one ( $\Sigma^0$  ( $\bar{\Sigma}^0$ )  $\rightarrow \Lambda$  ( $\bar{\Lambda}$ ) +  $\gamma$ ) with a 100 % branching ratio. Usually this feed-down contribution is not considered for the  $\Lambda$  ( $\bar{\Lambda}$ ) spectrum and as a consequence, model predictions for  $\Lambda$  ( $\bar{\Lambda}$ ) baryons are compared with data including secondary  $\Lambda$  ( $\bar{\Lambda}$ ) originated from  $\Sigma^0$  ( $\bar{\Sigma}^0$ ) [? ]. Thus the measurement of the  $\Sigma^0$  ( $\bar{\Sigma}^0$ ) spectrum enables us to estimate the contribution of the secondary  $\Lambda$  ( $\bar{\Lambda}$ ) in the hyperon spectrum. Furthermore, the  $\Sigma^0$  ( $\bar{\Sigma}^0$ ) production rates can be also an important measure to correct the  $p_T$  spectra of proton, pion and photon with taking into account the feed-down contributions from  $\Sigma^0$  ( $\bar{\Sigma}^0$ ) [? ].

Comparison of hyperon data with models as PYTHIA [3] and EPOS [4] permits to investigate their production mechanism. In particular, at LHC energies a significant disagreement was observed in  $p_T$  spectrum of  $\Lambda$  between PYTHIA6 Perugia 2011 [3] predictions and measurements of ALICE [5] and ATLAS [6] experiments. In this respect, the measurement of the  $p_T$  spectrum of  $\Sigma^0$  ( $\bar{\Sigma}^0$ ) and the ratio of  $\Sigma^0$  ( $\bar{\Sigma}^0$ ) to  $\Lambda$  ( $\bar{\Lambda}$ ) at the LHC energy are fundamental for the tuning of the models and to understand the hadronic mechanism processes.

In this paper the first measurement of the  $\Sigma^0$  ( $\bar{\Sigma}^0$ ) transverse momentum spectrum and its integrated yield measured at mid-rapidity with ALICE detector in inelastic pp collisions at  $\sqrt{s} = 7$  TeV are presented and compared with the  $\Lambda$  results in the same collisions. This enriches the existing data set limited until now to low energy collisions results.

## 2 Experimental setup and event selection

Since a complete and detailed description of the ALICE detector and of its performance during the LHC Run 1 (2010-2013) can be found in refs [7, 8], we briefly outline only the sub-detectors utilized for  $\Sigma^0$  analysis: Inner Tracking System (ITS), the Time Projection Chamber (TPC) and the VZERO-trigger detectors below.

Vertex reconstruction and tracking in the central-barrel and charged-hadron identification are performed with the Inner Tracking System (ITS) [7] and the Time-Projection Chamber (TPC) [9], which are located inside a solenoidal magnet providing a magnetic field of 0.5 T parallel to the LHC beam axis. The ITS is composed of six cylindrical layers of silicon detectors, located at radii between 4 and 43 cm from the nominal beam axis with covering a pseudo-rapidity range of  ~~$|\eta| < 0.9$~~   $|\eta| < 0.9$  ( ~~$< 2.0$  in L85?~~ What is correct?) and the full azimuth. The two innermost layers consist of Silicon Pixel Detectors (SPD), the two intermediate layers of Silicon Drift Detectors (SDD) and the two outermost layers of Silicon Strip Detector (SSD). The spatial resolution of the ITS enables measuring the distance of closest approach (DCA) of tracks to the primary vertex with a resolution in  $r\phi$ -plane better than  $75 \mu\text{m}$  in the transverse plane for  $p_T > 1$  GeV/c in pp collisions [10]. The Time Projection Chamber (TPC) is a large ( $90 \text{ m}^3$ ) cylindrical gaseous detector filled with a mixture of Ne/CO<sub>2</sub> /N<sub>2</sub> (85.7/9.5/4.8%). It covers radially between

85 and 250 cm from the beam axis and a pseudo-rapidity range of  $|\eta| < 0.9$  over the full azimuth, and provides track reconstruction with up to 159 space points, with a spatial resolution of ~~500  $\mu\text{m}$~~  500  $\mu\text{m}$  (to be checked) along the beam direction and in the transverse direction for tracks with  $\eta=0$  [9]. In addition, it enables particle identifications via the measurement of the specific ionization energy loss ( $dE/dx$ ) with a resolution of approximately 5.2% in pp collisions [8].

The data sample analyzed in this paper was recorded during the LHC pp run at  $\sqrt{s} = 7$  TeV in 2010 ~~(only 2010 or 2013?)~~ using a magnetic field of 0.5 T, with both field polarities and a minimum-bias (MB) trigger. The MB trigger required a single hit in the SPD detector or in one of the two VZERO counters, i.e. at least one charged particle anywhere in the  $\sim 8$  units of pseudo-rapidity covered by these detectors. In addition, a coincidence was required with signals from two beam pick-up counters, one on each side of the interaction region, indicating the passage of proton bunches. The trigger selection efficiency for inelastic collisions was estimated to be 85.2 % with a +6.2 % and ~~23 % uncertainty~~ 3.0 % uncertainty (ref?). While SPD covers  $|\eta| < 2.0$ , the two VZERO detectors, each consisting of scintillator tiles, are installed on both sides of the interaction point and cover  $-3.7 < \eta < -1.7$  and  $2.8 < \eta < 5.1$  [2, 11, 12].

JHSong will check and work:---

These VZERO detectors are used for triggering ~~(Is it the same to  $f_{inel}$ , which must be same to the  $MB_{OR}$  = INEL?)~~ and for rejecting beam-gas interactions ~~(What is it?)~~ (ref? ppMul.vs.LF paper). Due to the low luminosity of this ~~(Where can I find it?)~~ data taking a high-efficiency (85.2 % [13]) MB trigger ~~(It is NOT the MB, but  $MB_{OR}$ !)~~ was used. The contamination from beam-induced background was reduced to a negligible level with the help of the timing information of the VZERO counters and by a cut on the position of the primary vertex reconstructed by the SPD, as discussed in detail in [8] ~~(Is this related to  $N_{offlinetrigger}$ ? But how?)~~. The probability of collision pileup per triggered event was below ~~3-3.0~~ 3.0 % [12] ~~(How is it treated? Is it also taken into account for the final  $N_{norm}$ , but how?)~~. A total amount of about 500 million MB events has been utilized for the analysis.

Events used for the data analysis are further required to have just one reconstructed primary vertex (PV), events containing more than one distinct vertex are tagged as pileup and are discarded. The PV is determined by tracks reconstructed in the ITS and Time Projection Chamber (TPC), and track segments in the SPD [8]. MB events are selected when the PV is positioned along the beam axis within  $\pm 10$  cm from the center of the ALICE detector. The vertex reconstruction efficiency is 92.8 % [12].

Question: in [12],  $MB_{OR} = \text{INEL} = \text{at least one hit at SPD OR one of V0s}$

$NSD = \text{an additional condition of coincidence of two V0s} = MB_{AND}$

What was used?  $MB_{OR}$  or  $MB_{AND}$ ?

$MB_{AND}/MB_{OR} = 0.873$  in [10, 13]  $f_{inel} = \text{trigger efficiency for INEL} = 87\%$ ,  $f_{vtx} = \text{vertex reconstruction within } \pm 10\text{cm} = 88\%$

What is then  $N_{in}$  and  $N_{offlinetrigger}$ ? Nowhere I can find it.

what is the relation between  $N_{norm}$  and  $N_{MB}$ ?

---

### 3 Data analysis

$\Sigma^0$  were reconstructed by its electromagnetic decay ( $\Sigma^0 (\bar{\Sigma}^0) \rightarrow \Lambda (\bar{\Lambda}) + \gamma$ ) which has a 100 % branching ratio. ~~The main feature of this decay is the low energy of the energy of the emitted photon  $\approx 100$  MeV (any reference?)~~ The main feature of this decay is the low energy of the energy of the emitted photon due to small mass difference between  $\Sigma^0$  and  $\Lambda$ . The Photon Conversion Method (PCM) in the central tracking system was used for photon identification employing the ITS and the TPC [2, 8, 14]. It reconstructs and identifies the vertices ( $V0_\gamma$ ) of photon conversions to  $e^+e^-$  pair generated in the material of the inner detectors. For ALICE detector the probability of photon conversion in the central tracking system is about 0.08 and the reconstruction efficiency is about 0.67 [2]. Reliability of the method is based on the

good agreement of the actual material budget and the simulated one [8]. Then both the decay products of the  $\Sigma^0$  were identified as secondary vertices (V0):  $V0_\Lambda$  of the weak decay  $\Lambda(\bar{\Lambda}) \rightarrow p(\bar{p}) + \pi^+(\pi^-)$  and  $V0_\gamma$  of the photon conversion identified during tracking procedure as secondary vertices.

In the PCM analysis, photons are reconstructed as vertices ( $V0_\gamma$ ) of electron and positron pair [2, 14–16]. The tracks for  $e^-$  ( $e^+$ ) candidates are basically selected if: (1)  $|\eta| < 0.9$ , (2)  $p_T > 0.05$  GeV/c, (3) the ratio of the number of reconstructed to findable TPC clusters is larger than 0.35. For the particle identification of  $e^-$  ( $e^+$ ) tracks, the specific energy loss of electrons (positrons) in the TPC was required to be within a band between  $-6\sigma_e$  and  $7\sigma_e$  around the average  $dE/dx$ -value depending on  $p_T$ , where  $\sigma_e$  is a standard deviation of the measured  $dE/dx$  distribution for  $e^-$  ( $e^+$ ). In addition, in order to reduce pion and kaon contaminations by rejecting the tracks with  $|dE/dx| < 1\sigma_{\pi,K}$  for  $p_T < 0.5$  GeV/c, where  $\sigma_{\pi,K}$  are the standard deviations of measured  $dE/dx$  distribution for pions ( $\sigma_\pi$ ) and kaons ( $\sigma_K$ ), respectively.

To select photons among all secondary vertices, further selection was performed on the level of the reconstructed  $V0_\gamma$  [2, 14]. To remove  $\pi^0$  and  $\eta$  meson Dalitz decays, the transverse distance ( $R_T$ ) of  $V0_\gamma$  from PV have to be larger than 5 cm and smaller than 180 cm due to the V0 reconstruction procedure. Finally, the photons only with  $p_T > 0.020$  GeV/c and  $|\eta| < 0.9$  are accepted. Additional cuts of  $q_T = p_e \sin \Theta_{\gamma,e} < 0.06$  GeV/c, where  $p_e$  is electron momentum and  $\Theta_{\gamma,e}$  is the angle between  $\gamma$  momentum ( $p_\gamma$ ) and electron momentum [17], and  $\Psi_{pair} < 0.20$ , where  $\Psi_{pair}$  is the angle between the plane perpendicular to the magnetic field ( $x-y$ ) plane and the plane of the  $e^-$  ( $e^+$ ) pair [16] are applied for increasing the purity of  $e^-$  ( $e^+$ ) from  $\gamma$ .

To select  $\Lambda$  from  $\Sigma^0$ , the similar selection-criteria of the secondary vertex ( $V0_\Lambda$ ) used in [5, 18, 19] with exploiting the weak decay topology of  $\Lambda(\bar{\Lambda}) \rightarrow p\pi^-(\bar{p}\pi^+)$  (branching ratio of 63.9% and decay length of  $c\tau = 7.89$  cm [1]), is applied. The distance of closest approach (DCA) between positive (negative) tracks from  $V0_\Lambda$  and PV was selected to be larger than 0.06 cm, and the cosine of the pointing angle  $\Theta$  between the sum of daughter momenta and the line that connects the PV and  $V0_\Lambda$ , was requested to be greater than 0.993. The transverse distance between  $V0_\Lambda$  and PV is requested to be between 0.5 and 180 cm. An Armenteros-Podolanski cut on  $\Lambda$ :  $0.01 < \alpha < 0.17$  ( $\bar{\Lambda}$ ):  $0.01 < \alpha_\Lambda < 0.17$  and  $0.2 < |q_T| < 0.9$  was applied, where  $\alpha_\Lambda = \left| \frac{p_i^p - p_i^\pi}{p_i^p + p_i^\pi} \right|$ , where  $p_i^i$  is the longitudinal momentum of a particle  $i$  (p or  $\pi$ ) with respect to the  $\Lambda$  momentum direction,  $q_T$  corresponds to transverse momentum of proton with respect to the  $\Lambda$  momentum. Additionally a lifetime cut is applied as.... The  $\Lambda$  invariant mass ( $M_{p\pi}$ ) was selected within the interval of  $1.110 < M_{p\pi} < 1.120$  GeV/ $c^2$  to reduce the amount of combinatorial background of  $\Sigma^0$  invariant mass peak. Note, the nominal  $\Lambda$  mass ( $m_\Lambda$ ) with its uncertainty is  $m_\Lambda = 1115.683 \pm 0.006$  [1].

Missing points are: correct(!) definitions of  $\alpha$  and  $q_T$ , which have to be same to the analysis note. In the analysis note  $\alpha$

	$\gamma$	$\Lambda(\bar{\Lambda})$	$\Sigma^0(\bar{\Sigma}^0)$
$p_T$	$> 0.020$	$> 0.4$	$> 1.1$
$ \eta $	$< 0.9$	$< 0.5$ (0.9?)	$< 0.5$ for $\gamma$
$\alpha$	-	(0.01, 0.17) (0.01, 0.17)	$> 0.6$
$q_T$	$< 0.06$	(0.2, 0.9) (0.2, 0.9)	$< 0.12$

**Table 1:** The final selection criteria of  $\Sigma^0$  and its daughter particles.

In order to enhance the significance of the  $\Sigma^0$  signal, softer cuts on  $\Lambda$  selection than those used in  $\Lambda$  [18, 19] and the additional phase-space cuts on  $\Sigma^0$  as  $\alpha = \left| \frac{p_i^\gamma - p_i^\Lambda}{p_i^\gamma + p_i^\Lambda} \right| > 0.6$  and  $p_T < 0.12$ , ( $p_T$ ? or  $q_T$ ?)  $\alpha_{\Sigma^0} = \left| \frac{p_i^\gamma - p_i^\Lambda}{p_i^\gamma + p_i^\Lambda} \right| > 0.6$  and  $q_T < 0.12$ , are applied. Furthermore the  $\Sigma^0$  ( $\bar{\Sigma}^0$ ) rapidity range ( $|\eta|$  (not  $|\eta|$ ?)

less than 0.5 is selected for comparing directly with  $\Lambda$  results (ref?A paper in pp at 7TeV). The final ranges of the criteria are summarized in Table 1.

### 3.1 Signal extraction

The  $\Sigma^0 + \bar{\Sigma}^0$  signals were extracted from invariant-mass distributions in each  $p_T$ -bin of  $\Sigma^0$  for the range of 1.1 up to 8 GeV/c. For the estimates of raw yield of the signal, a Gaussian function added to a third-order polynomial is applied to describe the signal and background for the range of  $1.160 < M_{\Lambda\gamma} < 1.230$  GeV/c<sup>2</sup> in each  $p_T$ -bin. Examples of invariant mass distribution are presented in Fig. 1 for two different  $p_T$ -bins.

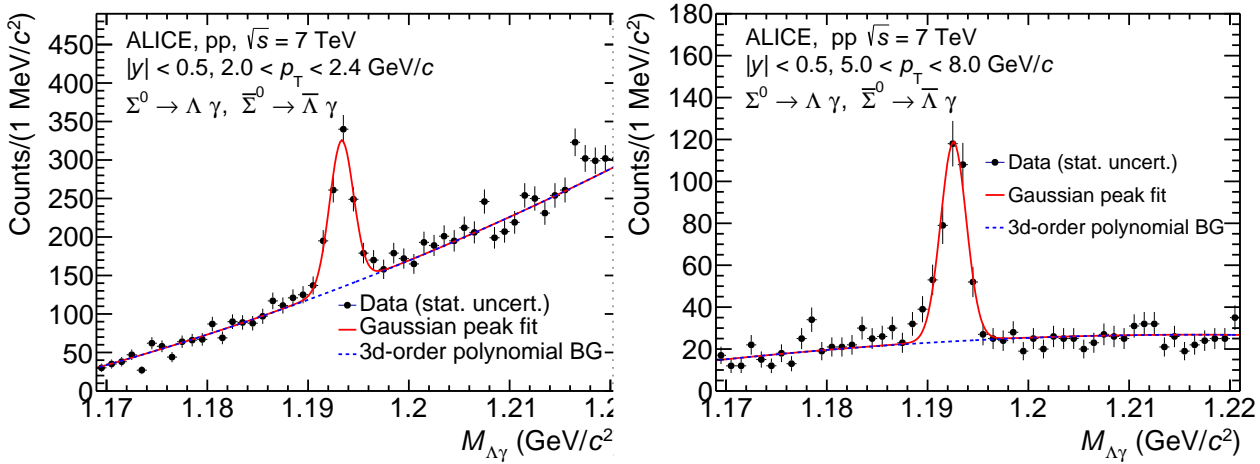


**Fig. 1:** Invariant mass distributions of  $\Lambda\gamma$  and  $\bar{\Lambda}\gamma$  pairs in  $p_T$  bins 2.0 – 2.4 and 5.0 – 8.0 GeV/c. The solid and dashed curves indicate a fit to the data using a third-order polynomial function with and without a Gaussian peak for the signal and background description, respectively.

The mean-value extracted peak position ( $M_{\Lambda\gamma} = 1192.94 \pm 0.035 \text{ MeV}/c^2$ ) of the  $\Sigma^0 + \bar{\Sigma}^0$  invariant masses from the fit results in all  $p_T$ -bins agrees well to the PDG value [1]:  $1192.642 \pm 0.024 \text{ MeV}/c^2$ . The standard deviations of the  $\Sigma^0$  signals extracted from the fits to data are about 2.2 MeV for  $1.1 < p_T < 1.6$  GeV/c and about 1.2 MeV-1.2 MeV (NOT matching with Analysis note Fig.12) for  $p_T > 2$  GeV/c, which are in a good agreement with the ones estimated by the fits to the simulated distributions. (How about then between 1.6 – 2 GeV/c?) The increase of the width at low  $p_T$  is mainly due to the low-energy photons.

The raw yield is obtained by integrating the Gaussian signal-fit function in the region  $\pm 3$  standard deviation in each  $p_T$  bin. The statistical uncertainties on the raw yields range between 3-6%. The different approaches with various signal and background estimations and the calculations of  $\Sigma^0$  yields are discussed for the systematic uncertainties in section 3.3.

### 3.2 Corrections and normalization

By using the PYTHIA6 Perugia-2011 event generator [3] and the GEANT 3.21 package [20], the  $\Sigma^0$  signals are counted in each  $p_T$  from a generated sample of about 542 million MB pp events, and the correction factors ( $A \times \epsilon$ ) are estimated-obtained from the ratio between the number of reconstructed and generated  $\Sigma^0$  hyperons in the same  $p_T$  and rapidity interval, also with taking account the vertex reconstruction efficiency. The  $p_T$  distribution of correction factors multiplied by branching ratios (B.R.) for  $\Sigma^0$  is shown in Fig. 2. The correction factors for  $\Sigma^0$  and  $\bar{\Sigma}^0$  are checked, respectively, and are consistent between each other in the measured  $p_T$ -interval between 1.1 and 8 GeV/c. Raw yields are thus

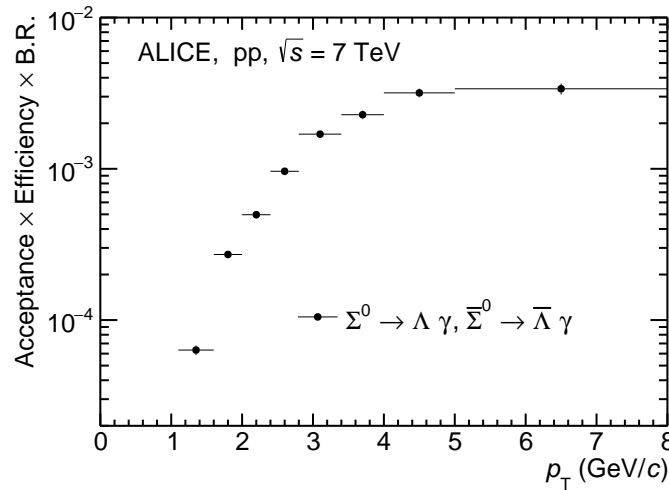


**Fig. 2:** The geometrical acceptance and the reconstruction efficiency ( $A \times \epsilon$ ) multiplied by B.R. for  $\Sigma^0$  in  $|y| < 0.5$  for MB events, obtained with PYTHIA6 Perugia-2011 event generator [3] ( $\bar{\Sigma}^0$  must be removed in the plot, since you say,  $\Sigma^0$  and  $\bar{\Sigma}^0$  are separately done and checked its consistency!). Only statistical uncertainties are shown.

corrected for the geometrical acceptance and the reconstruction efficiency ( $A \times \epsilon$ ) of the detector with taking into account the branching ratio of  $\Lambda$  decay.

The MB spectrum was normalized to the number of  $N_{norm}$  events after applying the correction factors for trigger efficiency and event selection including primary vertex reconstruction and rejection of pileup events. It was done analogous to the approach implemented in PCM package which was already used in several publications of ALICE [12, 14]. All those corrections result in a total scaling factor of 0.922 for the calculation of the total number of events used in Eq. 3.

The MB spectrum was normalized to the number of  $N_{norm}$  events after applying the correction factors for trigger efficiency and event selection including primary vertex reconstruction and rejection of pileup events. The yield of  $\Sigma^0$  as a function of  $p_T$  is after background subtraction  $N^{\Sigma^0}$ :

$$\frac{d^2N}{dp_T dy} = \frac{1}{N_{MB}} \frac{N^{\Sigma^0}}{\Delta y \Delta p_T} \frac{f_{vtx} \times f_{inel}}{A \epsilon}, \quad (1)$$

where  $N_{MB} = N_{in} - N_{OfflineTrigger}$  - trigger hits in either of two VZERO detectors, (Please specify what are  $N_{in}$ ,  $N_{OfflineTrigger}$ . Do you subtract also trigger hits in either of two VZERO detector??) the factor  $f_{vtx}$  (what is the value?) is the fraction of triggered events for which a good primary vertex is found,  $f_{inel}$  is the fraction of inelastic collisions that fulfill the trigger conditions. It was done analogous to the approach implemented in PCM package which was already used in several publications of ALICE [12, 14]. All those corrections result in a total scaling factor of 0.922 for the calculation of the total number of events used in Eq. 3.

Question: in [12],  $MB_{OR} = INEL$  = at least one hit at SPD OR one of V0s

NSD = an additional condition of coincidence of two V0s =  $MB_{AND}$

What was used?  $MB_{OR}$  or  $MB_{AND}$ ?

$MB_{AND}/MB_{OR} = 0.873$  in [10, 13]  $f_{inel}$  = trigger efficiency for INEL = 87%,  $f_{vtx}$  = vertex reconstruction within  $\pm 10$  cm = 88%

What is then  $N_{in}$  and  $N_{OfflineTrigger}$ ? Nowhere I can find it.

what is the relation between  $N_{norm}$  and  $N_{MB}$ ?

### 3.3 Systematic uncertainties



211 barlow-check comments The total  $\Sigma^0$  systematic uncertainty is determined by four general sources:

$$\sigma_{\text{syst}} = \sqrt{\sigma_{\gamma}^2 + \sigma_{\Lambda}^2 + \sigma_{\Sigma^0}^2 + \sigma_{\text{mat}}^2}, \quad (2)$$

212 where  $\sigma_{\gamma}$  and  $\sigma_{\Lambda}$  are the relative systematic uncertainties for the photon ( $\gamma$ ) and  $\Lambda$  ( $\bar{\Lambda}$ ) selections for the  
 213  $\Sigma^0$  ( $\bar{\Sigma}^0$ ) resonance, respectively, while  $\sigma_{\Sigma^0}$  and  $\sigma_{\text{mat}}$  are the systematic uncertainty due to the extraction  
 214 of  $\Sigma^0 + \bar{\Sigma}^0$  signals and the limited knowledge of the material budget for the conversion photon, relatively.  
 215 As two V0s for reconstruction of  $\Sigma^0 + \bar{\Sigma}^0$  resonances are independently analyzed with the photon con-  
 216 version ( $\gamma \rightarrow e^+e^-$ ) and the weak decay ( $\Lambda \rightarrow p + \pi^-$  and  $\bar{\Lambda} \rightarrow \bar{p} + \pi^+$ ), the corresponding systematic  
 217 uncertainties are fully independent. **Note, that quite low yield of the detected  $\Sigma^0 + \bar{\Sigma}^0$  limits the possi-**  
 218 **bility of the extraction of several components of the systematic uncertainties which were investigated in**  
 219 **stand-alone analysis of  $\Lambda$  and isolated photon production with much larger statistics.(Do we need this**  
 220 **argument? For what?)**

221 The main sources of systematic uncertainties for  $\Lambda$  selection are following: the pointing angle  $\Theta$ , V0 $_{\Lambda}$   
 222 positionradius, DCA between the  $\Lambda$  decay products, the ratio of the number of the reconstructed to the  
 223 findable TPC clusters and, **the difference between the proper lifetimes estimated from the difference**  
 224  **$L \frac{m^{\Lambda} - m^{K_S^0}}{p}$ , where  $L$  is defined as the distance between primary and V0 $^{\Lambda}$  vertex and  $p$  is its momen-**  
 225 **tum.(What is it? It was not mentioned before at all! The uncertainties of PID of daughter particles**  
 226 **MUST be included, instead.)** The relative systematic uncertainties estimated in this analysis for the  
 227  $\Lambda$  identification vary between 3 to 11 % depending  $p_T$ , see Table 2, and are consistent with the ones  
 228 estimated for  $\Lambda$  results in [5, 18].

229 The main source of the photon reconstruction uncertainty for PCM is determined by the identification of  
 230 V0 $^{\gamma}$ . The uncertainty of identification of  $e^+$  and  $e^-$  tracks is estimated with varying the restrictions of  $\sigma_e$   
 231 in the TPC relative to the nominal  $dE/dx$ , and the contamination criteria ( $\sigma_{\pi,K}$ ) of pions and kaons [2].  
 232 The limits of the accepted V0 $^{\gamma}$  were also varied to evaluate its stability. The contribution of photon  
 233 selection systematic uncertainty varies 4 to 12 % also depending  $p_T$ .

234 The systematic uncertainty of  $\Sigma^0 + \bar{\Sigma}^0$  yield extraction is estimated by varying the conditions of the back-  
 235 ground subtraction and raw-yield calculation of the invariant mass peaks shown in Fig. 1. The various  
 236 combinations of the signal and the background distributions estimated by a mixed-event ( $e^+e^- \Lambda - \gamma$   
 237 pairs from different events) and a second-order polynomial, and the bin-counting method are applied for  
 238 the for raw-yield extraction. The systematic uncertainties of raw-yield extraction range 2 to 10.5 %.

239 All systematic uncertainties are summarized in Table 2 for all  $p_T$ , and the mean value of the total sys-  
 240 tematic uncertainty averaged over all  $p_T$ -bins is 11.84 %.

Global track reconstruction error? Hadronic Interaction Error? etc?

$\sigma_{\Lambda}$	3 - 11 %
$\sigma_{\gamma}$	4 - 12 %
$\sigma_{\Sigma^0}$	2 - 10.5 %
Material budget	4.5 %
Total %	8 - 17

**Table 2:** Systematic uncertainties in  $\Sigma^0$  yield. The single valued uncertainties are  $p_T$  independent. Values given in ranges correspond to the minimum and maximum uncertainties.



## 4 Results and discussion

### 4.1 Transverse momentum spectrum

The corrected yield at mid-rapidity ( $dN/dy$ ) of  $(\Sigma^0 + \bar{\Sigma}^0)/2$  per event at mid-rapidity ( $dN/dy$ ) in  $p_T$  produced from inelastic pp collisions at 7 TeV is shown in Fig. 3. The measurements span the  $p_T$  range is from 1.1 to 8 GeV/c. It was checked that the spectra obtained separately for  $\Sigma^0$  and  $\bar{\Sigma}^0$  are equal inside the uncertainties.

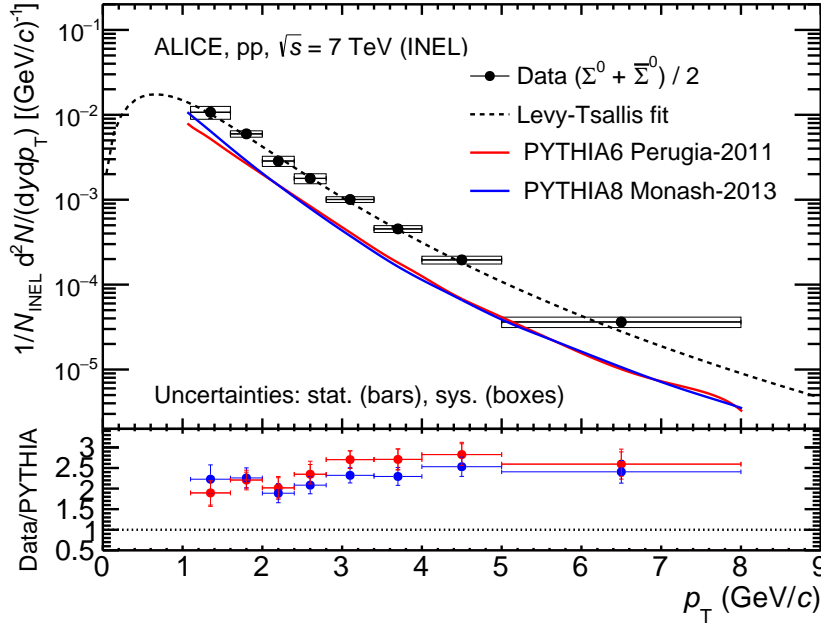


**Fig. 3:** (Top panel) Transverse momentum spectrum of  $(\Sigma^0 + \bar{\Sigma}^0)/2$  in the rapidity range  $|y| < 0.5$ . Statistical (bars) and systematic (boxes) uncertainties are included. The solid line represents Lévy-Tsallis fit, the dashed and dot-dashed lines (The figure must be updated for w/b (no color)) represents the spectrum from PYTHIA6 Perugia-2011 [3] and PYTHIA-8 Monash-2013 [21] generators. (Bottom panel) Ratio of  $(\Sigma^0 + \bar{\Sigma}^0)/2$  yield to the simulated ones for each generator in  $p_T$ .

The spectra are fitted with a Lévy-Tsallis function [22],

$$\frac{d^2N}{dp_T dy} = p_T \frac{dN}{dy} \frac{(n-1)(n-2)}{nC[nC + m_0(n-2)]} \left[ 1 + \frac{\sqrt{p_T^2 + m_0^2} - m_0}{nC} \right]^{-n}, \quad (3)$$

where  $m_0$  is the PDG value of  $m_{\Sigma^0}$  [1]. Free parameter of the fit are the  $n, C$  (nowhere defined) and  $dN/dy$ , which represents the particle yield per unit of rapidity. This fit function is widely used to describe all identified particle spectra in pp collisions[18, 23, 24], and to extract the integrated total yield for all  $p_T$ .

Finally, the integrated yield at mid-rapidity for  $\Sigma^0$  of  $dN/dy = 0.0256 \pm 0.0083_{(total)} = 0.0256 \pm 0.0038_{(stat)} \pm 0.0047_{(syst)} \pm 0.0057_{(extrap)}$  is obtained from the data for measured range ( $p_T > 1.1$  GeV/c) and the Lévy-Tsallis fit for unmeasured range ( $p_T < 1.1$  GeV/c (What about in high  $p_T$ ?)) of Fig. 3. The uncertainty (not shown (why?)) related to the overall normalization to inelastic events (or cross section) is fully correlated (with what?) and it amounts to +7.3% and -3.5 % (+6.2% and -3.0 %) [23, 25]. The value of the mean  $\langle p_T \rangle$  of  $\Sigma^0$  was taken from the result of the fit without the uncertainty on material budget (why? What is then with  $\sigma_{mat}$  as shown in Table ??? Isn't it included to the  $\sigma_{syst}$ ?):  $\langle p_T \rangle = 1.161 \pm 0.085 (\pm 0.076_{stat} \pm 0.038_{syst})$ .

The values of  $dN/dy$  and  $\langle p_T \rangle$  were calculated by using the experimental spectrum in the measured  $p_T$ -range and the Lévy-Tsallis fit function outside of the measured  $p_T$ -range. Note that the fraction of the fit-function in the unmeasured  $p_T$  region between 0 and 1.1 GeV, i.e. from the low- $p_T$  extrapolation to the total  $dN/dy$  is quite significant and equal to 0.58 from Lévy-Tsallis fit and 0.57 from Boltzmann-Gibbs Blast-Wave fit [26]. The uncertainty of the yield due to extrapolation to the unmeasured  $p_T$ -range was calculated by varying of the fit functions and is included as an independent source of the total uncertainty. The  $m_T$ -exponential,  $p_T$ -exponential, Fermi-Dirac, Boltzmann, Bose-Einstein Blast-Wave and Bose-Einstein fits [27, 28] are applied from the region of  $p_T = 0$  up to 4.0 GeV/c, where almost full statistics is presented. The weighted difference, with the weight corresponding to the probability of the fit, is used for the estimate of extrapolation uncertainty. (Fit functions are differently weighted? Why? Do we need this comment?) The fraction from the high- $p_T$  extrapolation is found to be negligible.

The transverse momentum spectra of  $(\Sigma^0 + \bar{\Sigma}^0)/2$  is compared to both the Perugia-2011 tune of the PYTHIA generator [3] and Monash-2013 tune [21], see Fig. 3. One can see that the applied generators significantly underestimate the  $dN/dy$  in  $p_T$ , accordingly the overall production of  $\Sigma^0$  and  $\bar{\Sigma}^0$ . Note that similar one is concluded from the comparison of  $\Lambda$  production at ALICE with PYTHIA Perugia-2011 event generator [18, 19]. (THERMUS MUST be compared and discussed!)

## 4.2 $\frac{\Sigma^0}{\Lambda}$ ratio

The ratios of  $(\Sigma^0 + \bar{\Sigma}^0)/2\Lambda$  from data [29] (this is for 13TeV! 7TeV is needed!), PYTHIA 6-Perugia 2011 [3] and PYTHIA 8-Monash 2013 [21] are presented as a function of  $p_T$  in Fig. 4. Note the trend of the monotonic increase of the ratio from data with  $p_T$ , while the ratios from both generators do show weird or practically no  $p_T$ -dependence. Despite of large uncertainties,  $\Sigma^0$  in low  $p_T$  is significantly suppressed relative to  $\Lambda$ . This ratio of  $\Sigma^0$  to  $\Lambda$  in high  $p_T$  in the generators is abnormally suppressed due to underestimated  $\Sigma^0$  and overestimated  $\Lambda$ -yields relative to the data, as shown in the previous section 4.1 and [29]. (THERMUS MUST be compared and discussed!)-

The integrated yield ratios of  $\Sigma^0$  to  $\Lambda$  from various collision systems at different energies are shown as a function of  $\sqrt{s}$  in Fig. 5. The integrated yield ratio measured with ALICE in pp collisions at  $\sqrt{s} = 7$  TeV is  $0.337 \pm 0.111$  (total) =  $0.337 \pm 0.051$  (stat)  $\pm 0.099$  (syst), where the extrapolation uncertainty is included into the systematic error. While yields of  $\Sigma^0$  have been measured in many different collision systems at low and intermediate energies, there exist only few results in high energy collisions including the ALICE result. The relatively new and more precise COSY-TOF pp data from Ref. [30, 31] see Fig. 5, have been published as the function of  $\varepsilon = \sqrt{s} - (m_p + m_K + m_{\Lambda, \Sigma^0})$  and correspond to  $\sqrt{s} \approx 2$  GeV/c. The cross section ratio  $\frac{\Sigma^0}{\Lambda} \approx 0.45 \pm 0.05$ .

The STAR detector reconstructed the electromagnetic decay ( $\Sigma^0 \rightarrow \Lambda + \gamma$ ) via the weak decay of the  $\Lambda \rightarrow p + \pi^-$  and  $\gamma$  conversions into  $e^+e^-$  pairs in the detector material [31, 32]. The cross section ratio  $\Sigma^0/\Lambda = 0.16^{+0.41}_{-0.09}$  was thus obtained in minimum bias 0.2 TeV d+Au collisions. Note that STAR data with so large errors were published only in a conference proceeding [32] by the collaboration due to the limited statistics. Note: The STAR result is, however, also cited in the regular paper [31] The most precise data are from L3 experiment [33, 34], where both  $\Sigma^0$  and  $\Lambda$  have been measured as a product of Z boson decays, as shown in Fig. 5, where  $\Sigma^0/\Lambda \approx 0.33 \pm 0.03$  (This value is hardly confirmed from the two papers [33, 34], and the phenomenology paper [31] DID NOT cite this L3 value!). These data in wide range of  $\sqrt{s}$  support the convergence of the  $\Sigma^0/\Lambda$ -ratio as expected by [31]. High energy nuclear collisions are of particular interest for the final state interactions [31] and the possibility of measuring isospin degeneracy factors from  $\Sigma^0$  and  $\Lambda$  yields and of opening new channels of hyperon production via partonic degrees of freedom [35].

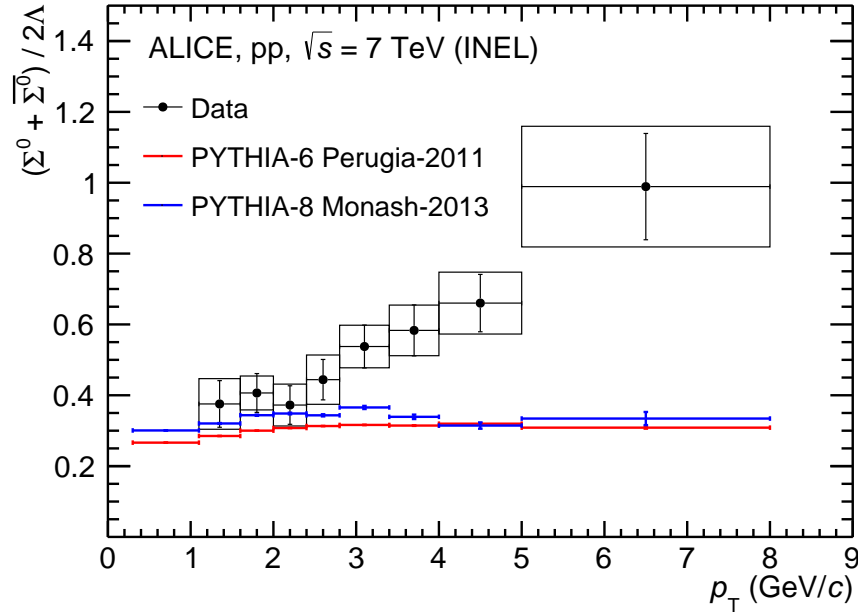


**Fig. 4:** The differential ratios of  $\Sigma^0 + \bar{\Sigma}^0)/2$  to  $\Lambda$  from data [29] in the same bins of  $p_T$  (blue points). (The ratio (line) from the Lévy-Tsallis curves based on  $\Sigma^0$  and  $\Lambda$  data is drawn in full range of  $p_T$ . ???) The red points indicate the same ratios from PYTHIA 6-Perugia 2011 and magenta points from PYTHIA 8-Monash 2013, respectively.

Any double counting of sys.error for the same cuts of daughter particle? These  $\Lambda$  are from 7TeV? or 13TeV?

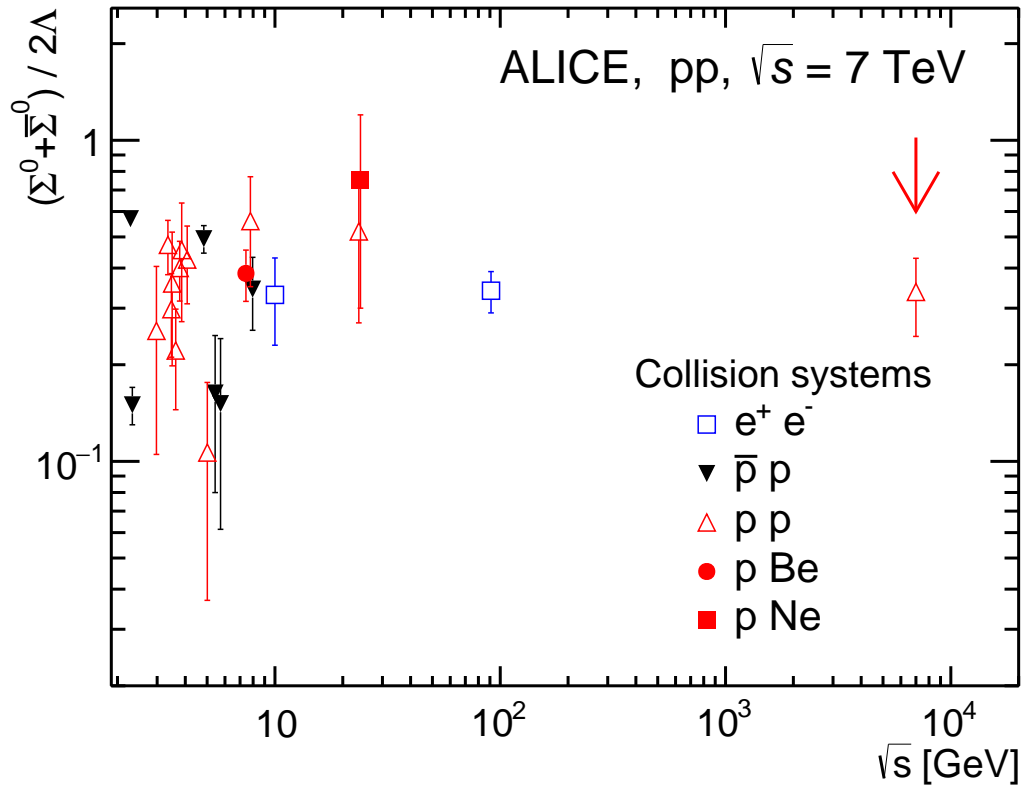


**Fig. 5:** Energy dependence of  $\Sigma^0$  to  $\Lambda$  cross section ratio Which points to include - to be discussed.

## 5 Conclusions

In summary,  $\Sigma^0$  ( $\bar{\Sigma}^0$ ) hyperons produced in pp collisions at  $\sqrt{s} = 7$  TeV are successfully reconstructed via electromagnetic decay to  $\Lambda$  ( $\bar{\Lambda}$ ) and  $\gamma$ . The  $p_T$  distribution of  $(\Sigma^0 + \bar{\Sigma}^0)/2$  is obtained and compared with two different versions of PYTHIA generators, which both significantly underestimate the differential yields. So far no generator is found to explain the  $\Sigma^0$  yield produced in pp collisions at  $\sqrt{s} = 7$  TeV. Furthermore the differential yield ratios of  $\Sigma^0$  to  $\Lambda$  from data and the generators are compared and the significant underestimates of  $\Sigma^0/\Lambda$  in both generators are observed in high  $p_T$ .

The integrated yield ratio measured in pp collisions at  $\sqrt{s} = 7$  TeV is  $(\Sigma^0 + \bar{\Sigma}^0)/2\Lambda = 0.337 \pm 0.111(\text{total}) = 0.337 \pm 0.051(\text{stat}) \pm 0.099(\text{syst})$ , where the systematic uncertainty includes the Lévy-Tsallis fits of  $\Sigma^0$  and  $\Lambda$  spectra extrapolated to the unmeasured low  $p_T$ . So far this  $(\Sigma^0 + \bar{\Sigma}^0)/2\Lambda$  at the highest energy collision system uniquely contributes to consistency of an isospin degeneracy factor, 1/3 with the same ratios in various collisions at different energies from world-wide experiments. The current measurement represents a relevant baseline for further investigation in p-Pb and Pb-Pb collisions.

## References

- [1] **Particle Data Group** Collaboration, K. Olive *et al.*, “Review of Particle Physics,” *Chin. Phys. C* **38** (2014) 090001.
- [2] **ALICE** Collaboration, B. Abelev *et al.*, “Neutral pion and  $\eta$  meson production in proton-proton collisions at  $\sqrt{s} = 0.9$  TeV and  $\sqrt{s} = 7$  TeV,” *Phys. Lett. B* **717** (2012) 162–172.
- [3] P. Skands, “Tuning Monte Carlo Generators: The Perugia Tunes,” *Phys.Rev.D* **82** (2010) 074018, arXiv:1005.3457v5 [hep-ph].
- [4] K. Werner, B. Guiot, I. Karpenko, and T. Pierog, “Analyzing radial flow features in  $p$ -Pb and  $p$ - $p$  collisions at several TeV by studying identified-particle production with the event generator EPOS3,” *Phys. Rev. C* **89** (2014) 064903.
- [5] **ALICE** Collaboration, D. Chinellato, “Strange and Multi-Strange Particle Production in ALICE,” (2012), arXiv:1211.7298.
- [6] **ATLAS** Collaboration, G. Aad *et al.*, “Kshort and Lambda production in pp interactions at  $\sqrt{s} = 0.9$  and 7 TeV measured with the ATLAS detector at the LHC,” *Phys. Rev. D* **85** (2012) 012001, arXiv:1111.1297 [hep-ex].
- [7] **ALICE** Collaboration, K. Aamodt *et al.*, “The ALICE experiment at the CERN LHC,” *JINST* **3** (2008) S08002.
- [8] **ALICE** Collaboration, B. Abelev *et al.*, “Performance of the ALICE Experiment at the CERN LHC,” *Int. J. Mod. Phys. A* **29** (2014) 1430044, arXiv:1402.4476 [nucl-ex].
- [9] **ALICE** Collaboration, J. Alme *et al.*, “The ALICE TPC, a large 3-dimensional tracking device with fast readout for ultra-high multiplicity events,” *NIM A* **622** (2010) 316, arXiv:1001.1950 [physics.ins-det].
- [10] **ALICE** Collaboration, B. Abelev *et al.*, “Measurement of charm production at central rapidity in proton-proton collisions at  $s = 7$  TeV,” *JHEP* **01** (2012) 128, arXiv:1111.1553 [hep-ex].
- [11] **ALICE** Collaboration, K. Aamodt *et al.*, “Charged-particle multiplicity measurement in proton-proton collisions at  $\sqrt{s} = 7$  TeV with ALICE at LHC,” *Eur. Phys. J. C* **68** (2010) 345–354, arXiv:1004.3514 [nucl-ex].
- [12] **ALICE** Collaboration, B. Abelev *et al.*, “Inclusive photon production at forward rapidities in proton-proton collisions at  $\sqrt{s} = 0.9, 2.76$  and 7 TeV,” *Eur. Phys. J. C* **75** (2015) 146, arXiv:1411.4981 [nucl-ex].
- [13] **ALICE** Collaboration, B. Abelev *et al.*, “Measurement of inelastic, single- and double-diffraction cross sections in protonproton collisions at the LHC with ALICE,” *Eur. Phys. J. C* **73** (2013) 2456, arXiv:1208.4968 [hep-ex].
- [14] **ALICE** Collaboration, J. Adam *et al.*, “Direct photon production in Pb-Pb collisions at  $\sqrt{s_{NN}} = 2.76$  TeV,” *Phys. Lett. B* **754** (2016) 235–248, arXiv:hep-ph/0608098.
- [15] **ALICE** Collaboration, B. Abelev *et al.*, “Neutral pion production at midrapidity in pp and Pb-Pb collisions at  $\sqrt{s_{NN}} = 2.76$  TeV,” *Eur. Phys. J. C* **74** (2014) 3108, arXiv:1311.0633 [nucl-ex].
- [16] **ALICE** Collaboration, S. Acharya *et al.*, “Neutral pion and  $\eta$  meson production in p-Pb collisions at  $\sqrt{s_{NN}} = 5.02$  TeV,” arXiv:1801.07051 [nucl-ex].

- [17] J. Podolanski and R. Armenteros, “III Analysis of V-events,” *Philos. Mag.* **45** (360) (1954) 13–30.
- [18] **ALICE** Collaboration, K. Aamodt *et al.*, “Strange particle production in proton-proton collisions at  $\sqrt{s} = 0.9$  TeV with ALICE at the LHC,” *Eur. Phys. J.* **C71** (2011) 1594, arXiv:1012.3257 [nucl-ex].
- [19] **ALICE** Collaboration, J. Adam *et al.*, “Multiplicity dependence of pion, kaon, proton and lambda production in p–Pb collisions at  $\sqrt{s_{NN}} = 5.02$  TeV,” *Phys. Lett.* **B728** (2014) 25–38, arXiv:1307.6796 [nucl-ex].
- [20] R. Brun, F. Carminati, and S. Giani, “GEANT detector description and simulation tool,” *CERN-W5013* (1994) .
- [21] R. Skands, S. Carrazza, and R. J., “Tuning PYTHIA 8.1: the Monash 2013 Tune ,” *Eur. Phys. J.* **C 74** (2014) 3024–1468, arXiv:hep-ph/1404.5630.
- [22] C. Tsallis, “Possible generalization of Boltzmann-Gibbs statistics,” *J. Statist. Phys.* **52** (1988) 479–487.
- [23] **ALICE** Collaboration, B. Abelev *et al.*, “Production of  $\Sigma(1385)^\pm$  and  $\Xi(1530)^0$  in proton-proton collisions at  $\sqrt{s} = 7$  TeV,” *Eur. Phys. J.* **C75** (2015) 1, arXiv:1406.3206 [nucl-ex].
- [24] **ALICE** Collaboration, J. Adam *et al.*, “Production of  $K^*(892)^0$  and  $\phi(1020)$  in p–Pb collisions at  $\sqrt{s_{NN}} = 5.02$  TeV,” *Eur. Phys. J.* **C76** (2016) 245, arXiv:1601.7868 [nucl-ex].
- [25] **ALICE** Collaboration, B. Abelev *et al.*, “Measurement of inelastic, single- and double-diffraction cross sections in proton-proton collisions at the LHC with ALICE ,” *Eur. Phys. J.* **C73** (2013) 2456, arXiv:1208.4968 [hep-ex].
- [26] E. Schnedermann, J. Sollfrank, and U. Heinz, “Thermal phenomenology of hadrons from 200A GeV S+S collisions,” *Phys. Rev.* **C48** (1993) 2462–2475, nucl-th/9307020.
- [27] **STAR** Collaboration, B. I. Abelev *et al.*, “Systematic measurements of identified particle spectra in pp, d–Au, and Au–Au collisions at the STAR detector,” *Phys. Rev.* **C79** (2009) 034909.
- [28] **STAR** Collaboration, J. Adams *et al.*, “ $K(892)^*$  resonance production in Au–Au and pp collisions at  $\sqrt{s_{NN}} = 200$  GeV,” *Phys. Rev.* **C71** (2005) 064902, nucl-ex/0412019v2.
- [29] **ALICE** Collaboration, X. XXX *et al.*, “Production of light flavor hadrons in pp collisions at  $\sqrt{s} = 13$ TeV, IN DEVELOPMENT,” *Eur. Phys. J.* **??** (2017) ??–??
- [30] **COSY-TOF** Collaboration, M. Abdel-Bary *et al.*, “Production of Lambda and Sigma<sup>0</sup> hyperons in proton-proton collisions ,” *Eur. Phys. J.* **A 46** (2010) 27–44, arXiv:1008.4287 [nucl-ex].
- [31] A. Sibirtsev, J. Haidenbauer, H. Hammer, and U.-G. Meißner, “Phenomenology of the  $\Lambda/\Sigma$  production ratio in pp collisions ,” *Eur. Phys. J* **A 29** (2006) 363–367, arXiv:1008.4287 [nucl-ex].
- [32] **STAR** Collaboration, G. V. Buren, “The Ratio  $\Sigma^0/\Lambda$  at RHIC ,” *Rom. Rep. Phys.* **58** (2006) 069–074, nucl-ex/0512018.
- [33] **L3** Collaboration, M. Acciarri *et al.*, “Inclusive Sigma+ and Sigma0 Production in Hadronic Z Decays ,” *Phys.Lett.* **B479** (2000) 79–88, hep-ex/0002066.
- [34] **L3** Collaboration, M. Acciarri *et al.*, “Measurement of inclusive production of neutral hadrons from Z decays ,” *Phys.Lett.* **B328** (1994) 223–233.

- 396 [35] J. R. P. Koch, “Time evolution of strange-particle densities in hot hadronic matter ,” *Nucl. Phys. A*  
397 **444** (1985) 678–691.



**A The ALICE Collaboration**